Radioimmunotherapy of Solid Tumors by Targeting Extra Domain B Fibronectin: Identification of the Best-Suited Radioimmunoconjugate

Dietmar Berndorff,[1] Sandra Borkowski,[1] Stephanie Sieger,[1] Axel Rother,[2] Matthias Friebe,[1] Francesca Viti,[3] Christoph S. Hilger,[1] John E. Cyr,[1] and Ludger M. Dinkelborg[1]

Abstract

Purpose: The expression of extra domain B (ED-B) fibronectin is always associated with angiogenic processes and can be exclusively observed in tissues undergoing growth and/or extensive remodeling. Due to this selective expression, ED-B fibronectin is an interesting target for radioimmunotherapy of malignant diseases. The aim of this study was to identify the most appropriate ED-B-targeting radioimmunoconjugate for the therapy of solid tumors.

Experimental Design: Three ED-B fibronectin-binding human antibody formats of L19 were investigated: dimeric single-chain Fv (~50 kDa), "small immunoprotein" (SIP, ~80 kDa), and immunoglobulin G1 (IgG1, ~150 kDa). These L19 derivatives were either labeled with I-125 or with In-111 (using MX-diethylenetriaminepentaacetic acid, MX-DTPA). Pharmacokinetics and tumor accumulation of the radiolabeled immunoconjugates were investigated in F9 (murine teratocarcinoma) tumor-bearing mice. Subsequently, dosimetry for the corresponding therapeutic isotopes I-13-1 and Y-90 was done. After testing the myelotoxicity of I-131-L19-SIP and I-131-L19-IgG1 in non-tumor-bearing mice, the therapeutic efficacy of these iodinated antibody formats was finally investigated in F9 tumor-bearing mice.

Results: The most favorable therapeutic index was found for I-131-L19-SIP followed by I-131-L19-IgG1. The therapeutic index of all In-111-labeled derivatives was significantly inferior. Considering the bone marrow as the dose-limiting organ, it was calculated that activities of 74 MBq I-131-L19-SIP and 25 MBq I-131-L19-IgG1 could be injected per mouse without causing severe myelotoxicity. The best therapeutic efficacy was observed using I-131-L19-SIP, resulting in significant tumor growth delay and prolonged survival after a single injection.

Conclusion: Compared with other L19-based radioimmunoconjugates, I-131-L19-SIP is characterized by superior antitumor efficacy and toxicity profile in the F9 teratocarcinoma animal model. These results indicate that ED-B fibronectin-targeted radioimmunotherapy using I-131-L19-SIP has potential to be applied to treatment of solid cancers.

Radioimmunotherapy using systemically administered radiolabeled antibodies is an interesting approach to metastatic cancer treatment. Promising results have been reported in patients with hematologic malignancies, presumably due to their high intrinsic radiosensitivity and a relatively good access of the radiolabeled antibodies to the cancer cells (1, 2). Solid cancers, however, have proved to be far less sensitive to this form of treatment due to several reasons, including a limited vascular supply, heterogeneous uptake of the antibody and elevated interstitial pressure in combination with a relatively long transport distance in the interstitium (3). Several approaches have been tried to overcome these problems, including use of small molecular weight fragments that target tumors faster (4) or alternatively, the use of intact antibodies that can be modified for use in pretargeting protocols (5–7). Thus far, however, remissions in solid tumors have been partial, infrequent, and short-lived (8). Consequently, new approaches will be needed to hopefully overcome the impediments to successful radioimmunotherapy.

The extra domain B (ED-B) of fibronectin consists of 91 amino acids that are identical in mouse, rat, rabbit, dog, monkey, and man (9). This domain arises by alternative splicing in the fibronectin molecule exclusively at sites of tissue remodeling and is one of the few angiogenesis markers known thus far. A number of human antibodies to ED-B have been isolated using different technologies (10, 11). In particular, L19 is a human single-chain Fv antibody fragment with subnanomolar affinity to ED-B (12), which has been shown to efficiently localize on tumoral neovasculature both in animal models (13, 14) and in cancer patients (15). Several derivatives of L19 have already been described that selectively deliver

Authors' Affiliations: [1]Schering AG Research Laboratories, Berlin, Germany; [2]Forschungszentrum Rossendorf e.V., Institut für Bioorganische und Radiopharmazeutische Chemie, Dresden, Germany; and [3]Philogen S.p.A, Monteriggioni-Siena, Italy

Presented at the Tenth Conference on Cancer Therapy with Antibodies and Immunoconjugates, October 21-23, 2004, Princeton, New Jersey.

Requests for reprints: Dietmar Berndorff, Schering AG, Research Laboratories, 13342 Berlin, Germany. Phone: 49-30-46817555; Fax: 49-30-46816609. E-mail: dietmar.berndorff@schering.de.

doi:10.1158/1078-0432.CCR-1004-0015

therapeutically efficacious molecules to the tumor vasculature in preclinical animal models (16–20).

In this article, we report on a novel approach for radioimmunotherapy of solid tumors by making use of ED-B fibronectin targeting. ED-B fibronectin is accessible from the blood stream because its expression is predominantly vessel associated during angiogenesis. Compared with the targeting of receptors that are expressed on the tumor cell surface, the delivery of ionizing radiation mainly to the tumor vasculature might lead to an improved therapeutic efficacy by destroying the tumor's vascular supply.

To determine the best-suited radioimmunoconjugate for ED-B-targeted radioimmunotherapy, a series of experiments was designed. First, three human antibody formats of L19 [i.e., dimeric single-chain Fv (~50 kDa), "small immunoprotein" (SIP; ~80 kDa), and immunoglobulin G1 (IgG1, ~150 kDa)] were labeled with I-125 and In-111 (MX-DTPA), respectively. Each of the labeled immunoconjugates was carefully analyzed *in vitro* for labeling efficiency, radiochemical purity, and immunoreactivity. Subsequently, the biodistributions of these radioimmunoconjugates were studied *in vivo* after i.v. injection in the s.c. syngeneic F9 teratoma nude mouse model. Based on the biodistribution results, doses for mouse organs and for tumor, the maximum tolerable activity (MTA), and the resulting therapeutic index (i.e., the dose ratio between the tumor and the dose-limiting organ) for the corresponding radiotherapeutic immunoconjugates labeled with I-131 and Y-90 were estimated. To confirm the predicted MTA of I-131-L19-SIP and I-131-L19-IgG1, the myelotoxicity of both compounds was investigated after injection in non-tumor-bearing mice. Finally, the therapeutic efficacy of I-131-L19-SIP and I-131-L19-IgG1 was studied in F9 tumor-bearing mice.

Materials and Methods

Cell culture and animals. Mouse embryonal teratocarcinoma cells (F9) were kindly provided by Dario Neri (Swiss Federal Institute of Technology, Zurich, Switzerland). Tumor cells were cultivated in DMEM with Glutamax supplemented with 10% FCS (all reagents from Invitrogen, Karlsruhe, Germany) and maintained at 37°C and 5% CO_2.

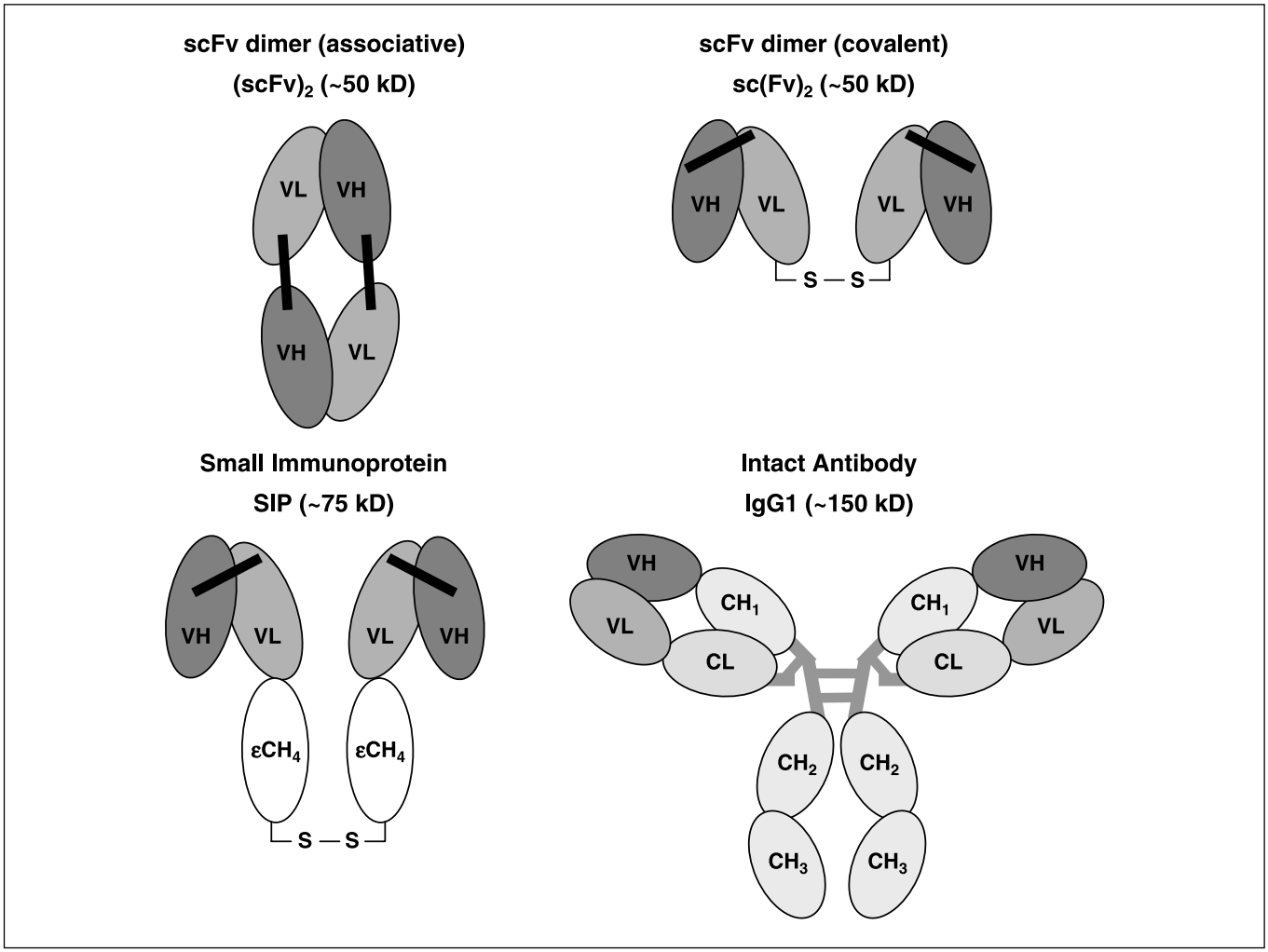

Fig. 1. Schematic drawing shows the domain structure of all antibody formats that were investigated in this study. The derivatives of this study are consisting of V_L and V_H domains of L19 scFv. The covalent scFv dimer is formed by an intermolecular disulfide bridge after recombinant insertion of the peptide sequence $(Gly)_3$-Cys-Ala at the C-OH-terminal end of L19 scFv. In the SIP molecule, the dimerization of V_L and V_H domains of L19 scFv is achieved by recombinant connection of the L19 scFv to the εCH4 domain of the human IgE secretory isoform IgE-S2. The intact antibody is formed by recombinant connection of the L19 heavy and light chain to the complete human γ1 constant heavy and the human constant κ light chain, respectively.

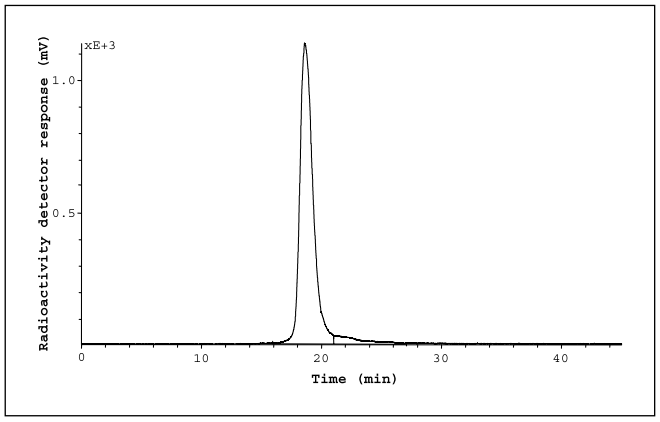

Fig. 2. SE-HPLC (radiation detection) of I-125-L19-SIP.

To induce tumors, female nude mice (NMRI-Foxn1^{nu}) weighing 20 to 25 g and purchased from Taconic Europe (Bomholtgard, Denmark) were s.c. injected with 1×10^6 F9 cells in a volume of 100 μL PBS into the right hind limb. Biodistribution experiments were carried out after 10 to 12 days when tumors reached a mass of 100 to 300 mg. For therapy experiments, mice with palpable tumors of 50 to 100 mm^2 were used after 7 to 9 days of tumor growth. All animal experiments were done in compliance with the German law on the Protection of Animals.

Antibody expression, purification, and radiolabeling. Single-chain Fv (L19), SIP (L19), and IgG1 (L19) were expressed and purified by immunoaffinity chromatography as described earlier (21). Expression and purification of the single-chain Fv AP39, which has been generated by insertion of the peptide sequence $(Gly)_3$-Cys-Ala at the COOH-terminal end of the V_L chain of single-chain Fv (L19), was done according to a procedure described elsewhere.[4] Both the single-chain Fv (L19) and AP39 used in this study were dimeric single-chain Fv molecules, either due to associative interactions (L19) or because of an intermolecular disulfide bridge (AP39). All antibody formats used in this study are schematically shown in Fig. 1. It has been shown that different L19-based antibody formats have a similar binding affinity when measurements are done with the antigen in solution to avoid avidity effects (22). However, when the antigen is bound to a solid phase, bivalent L19-based antibody formats show better performance due to slow disassociation rates (22).

Radioiodination of antibodies and antibody fragments was done following a slightly modified version of the original IODO-GEN method (23) using IODO-GEN precoated iodination tubes (Pierce, Rockford, IL). For the reported biodistribution studies, 200 μg of protein in 500 μL of PBS were labeled with 0.5 mCi of NaI-125 (Amersham Biosciences, Little Chalfont, United Kingdom). For the therapy studies, 1,000 μg protein in 1,000 μL of PBS were labeled with 20 mCi of NaI-131 (Amersham Buchler, Braunschweig, Germany). After incubation at room temperature for 15 minutes, the radiolabeled protein was separated from free radioiodine by gel filtration using NAP5 columns (Amersham Biosciences, Uppsala, Sweden) for I-125 labelings and PD10 columns (Amersham Biosciences, Uppsala, Sweden) for I-131 labelings. The columns were pretreated with 0.5% bovine serum albumin (BSA) in PBS and equilibrated and eluted with PBS. For NAP5 columns, 1 mL fractions, and for PD10 columns, 3.5 mL fractions, were collected. The radioactivity of the fractions was measured with a dose calibrator (MED Nuclear-Medizintechnik Dresden GmbH, Dresden, Germany).

The purity of the radiolabeled proteins was analyzed by SDS-PAGE using Gradient 10-15 Phast gels and a Phast System (Pharmacia, Uppsala, Sweden) followed by autoradiography using a Phosphorimager (Molecular Dynamics, Krefeld, Germany). I-125-labeled BSA and I-125-labeled carbonic anhydrase were used as standards. Size exclusion high pressure liquid chromatography (SE-HPLC) was done on a HPLC-pump 64 (Knauer, Berlin, Germany) equipped with a LB 507 B radiation detector (EG&G Berthold, Bad Wildbach, Germany) using a TSK-gel column SWxL, 50 × 6 mm (Tosoh Haas, Montgomeryville, PA) with TSK buffer as mobile phase (0.1 mol/L Na_2HPO_4, 0.1 mol/L Na_2SO_4, 0.05 mol/L NaN_3) and a flow rate of 0.5 mL/min.

The immunoreactivity of the radioimmunoconjugates was determined using a test column comprised of a Pasteur pipette filled with 250 μL ED-B Sepharose resin (24) and saturated with 0.5% BSA in PBS. The test column was loaded with ~0.2 MBq radiolabeled protein in 500 μL of 0.5% BSA in PBS and rinsed with 2 × 500 μL 0.5% BSA in PBS to remove the non-immunoreactive protein fraction. The immunoreactive protein fraction was then eluted with 2 × 750 μL of aqueous triethylamine solution (0.1 mol/L). Both, the radioactivity of the fractions and that remaining on the column, were measured with a dose calibrator and the immunoreactivity was calculated as the percent radioactivity bound to the column or in the immunoreactive fraction.

MX-DTPA isothiocyanate (4-*p*-benzylisothiocyanato-8-methyl-3,6,9-triaza-3*N*,6*N*,9*N*-tricarboxymethyl-1,11-undecanoic acid) for conjugation to the proteins was synthesized according to the literature (25, 26).

Subsequent conjugation of MX-DTPA isothiocyanate to the ε-amine group of lysine residues of the L19-based antibody derivatives AP39, L19-SIP, and L19-IgG1, and labeling of the proteins with In-111 (Amersham Health, Little Chalfont, United Kingdom) were conducted according to described procedures (27). For example, 3.6 nmol of AP39 in sodium borate buffer (80 μL, 0.1 mol/L, pH 8.5) were added to 50 μg of MX-DTPA isothiocyanate (1 mg/mL in sodium borate buffer, 0.1 mol/L, pH 8.5), and the mixture was incubated for 1 hour at 37°C. Subsequently, the sample was dialyzed thrice (2 × 1 hour, 1 × overnight) using a Slide-A-Lyzer (10,000 molecular weight cut-off membrane; Pierce) and sodium acetate buffer (0.1 mol/L, pH 6) and stored at 4°C until use. For In-111 radiolabeling, 28 MBq of [In-111] $InCl_3$ (in HCl, 0.1 mol/L) were added to the AP39-MX-DTPA conjugate. After incubation at room temperature for 30 minutes, the radiolabeled product was purified on a NAP5 column as described above for the radioiodinated products. The purity of the In-111 radiolabeled conjugates was evaluated by SE-HPLC, immunoreactivity, and SDS-PAGE.

Biodistribution experiments. Mice were i.v. injected with 37 to 74 kBq of the labeled antibody formats into the tail vein in a total

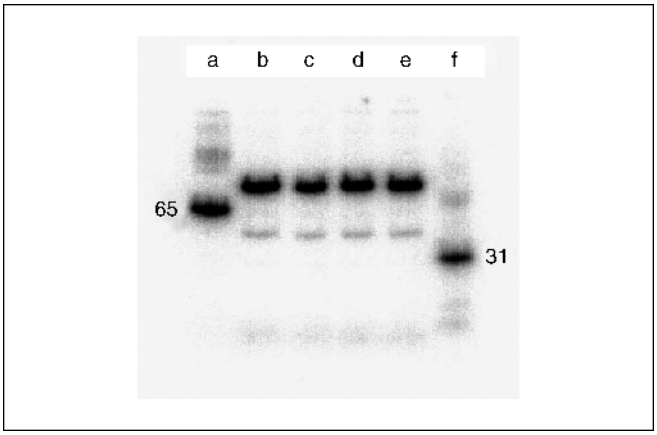

Fig. 3. Autoradiogram of a SDS-PAGE of I-125-L19-SIP: I-125-labeled BSA (*lane a*), I-125-L19-SIP (*lanes b* and *c*), I-125-L19-SIP heated for 4 minutes at 95 °C (*lanes d* and *e*), and 125-labeled carbonic anhydrase (*lane f*). Molecular weights of I-125-labeled BSA and I-125-labeled carbonic anhydrase are given in kDA.

[4] In preparation.

volume of 50 to 100 μL. At least four different time points with three mice per time point were investigated after a single injection of the radioactive compounds. At predetermined time points (0.25-24 hours for small antibody formats, 4-96 hours for larger formats), animals were sacrificed by decapitation. The dissected organs and collected excretions were counted for radioactivity in a γ-counter (Compugamma, LKB Wallac, Turku, Finland) and values of % injected dose/g and % injected dose were calculated.

Mouse dosimetry. Doses for mouse organs were estimated based on medical internal radiation dose (28) using the biodistribution results of the labeled antibody formats. Using I-125 and In-111 as surrogates, dosimetric calculations were made for the corresponding therapeutic isotopes I-131 and Y-90. The following assumptions in accordance to medical internal radiation dose were used: (a) uniform distribution of radioactivity within the organs, (b) organ shapes as spheres, (c) linear interpolation of *S* values. Residence times were calculated and isotope-specific *S* values were linearly interpolated depending on the mouse organ masses to obtain tumor and organ doses in mGy/MBq (29). Only self-to-self doses but not cross-fire effects were taken into account. The red marrow doses were estimated based on a method by Sgouros (30) assuming a red marrow-to-blood activity concentration ratio of 0.36. Regarding the dose-limiting organ, which was either the red marrow or the kidneys depending on the antibody format, maximum activities to be injected per mouse were determined based on published human tolerance doses of $TD_{50/5}$ = 4.5 Gy for the red marrow and $TD_{50/5}$ = 25 Gy for the kidneys (31). These MTAs per mouse were used to calculate absolute tumor doses (in Gy) for a 100-mg normalized tumor mass in relation to the respective dose-limiting organ (therapeutic index).

Determination of blood counts. To confirm the calculated MTAs of I-131-L19-SIP or I-131-L19-IgG1 that can be injected into a mouse without causing irreversible bone marrow toxicity, non–tumor-bearing mice were injected with increasing doses of iodinated antibody (25-74 MBq). The total and differential leukocyte and thrombocyte numbers were counted before injection of radioiodinatated antibody and at weekly intervals thereafter. Approximately 100 μL of blood were collected by retro-orbital bleeding in EDTA-coated microtubes (Sarstedt, Nuembrecht, Germany). Samples were counted using the Hematology Analyzer Advia 120 (Bayer-Diagnostik, Munich, Germany).

Radioimmunotherapy. Tumor sizes were monitored by measurement of the length and width of the tumor using calipers immediately before therapy started and thrice per week thereafter. Tumor-bearing mice were either injected with NaCl (controls) or with a single dose (25-74 MBq) of the radiolabeled antibodies I-131-L19-SIP or I-131-L19-IgG1. The maximum activity injected per mouse was determined earlier by dosimetry calculations and confirmed by myelotoxicity studies. All treatment groups consisted of n = 6 to 10 animals. In a

Table 1. Biodistribution of I-125-labeled anti-ED-B antibody formats in F9 tumor-bearing mice each at two selected time points

Format	L19 $(scFv)_2$, mean (SD)		L19-SIP, mean (SD)		L19-IgG1, mean (SD)	
Time points	1 h	24 h	5 h	24 h	24 h	96 h
Uptake in % ID/g						
Spleen	2.3 (0.5)	0.2 (0.0)	3.2 (0.4)	0.8 (0.1)	1.9 (0.5)	0.5 (0.4)
Liver	1.8 (0.2)	0.1 (0.0)	2.6 (0.3)	0.5 (0.1)	1.8 (0.4)	0.2 (0.1)
Kidneys	27.7 (5.4)	1.5 (0.8)	6.9 (3.5)	1.0 (0.1)	1.5 (0.5)	0.3 (0.2)
Lung	4.8 (0.3)	0.7 (0.3)	7.2 (1.9)	1.4 (0.4)	3.6 (1.0)	0.4 (0.3)
Bone	3.2 (0.5)	0.8 (0.1)	5.8 (0.4)	1.9 (0.6)	5.5 (1.9)	0.9 (1.0)
Thyroid	54.6 (39.1)	214.9 (35.4)	132.4 (46.8)	569.8 (297.7)	80.0 (78.3)	152.2 (78.6)
Muscle	1.2 (0.4)	0.6 (0.8)	0.8 (0.1)	0.3 (0.0)	0.4 (0.1)	0.2 (0.2)
Tumor	8.6 (2.6)	3.4 (2.3)	18.4 (1.8)	12.6 (5.0)	13.0 (5.0)	3.9 (3.1)
Blood	4.7 (0.5)	0.4 (0.0)	8.6 (0.5)	1.5 (0.1)	4.9 (1.9)	0.7 (0.9)
Ovaries	7.0 (2.8)	1.3 (0.4)	11.6 (3.3)	3.1 (0.6)	8.5 (3.3)	1.8 (1.8)
Uterus	4.2 (0.7)	0.8 (0.3)	8.6 (2.6)	7.3 (1.8)	10.4 (5.7)	2.9 (3.5)
Tumor/Tissue ratios						
T/Spleen	3.7 (0.5)	14.1 (8.0)	5.8 (1.3)	15.8 (5.1)	7.5 (4.3)	9.0 (4.6)
T/Liver	4.6 (0.9)	25.6 (18.1)	7.2 (1.5)	29.7 (18.0)	7.2 (1.7)	19.3 (1.8)
T/Kidneys	0.3 (0.1)	2.6 (2.1)	3.2 (1.5)	13.3 (5.9)	8.6 (0.4)	16.8 (9.2)
T/Lung	1.8 (0.5)	5.2 (3.1)	2.7 (0.9)	9.6 (4.5)	3.5 (0.5)	8.4 (1.6)
T/Bone	2.6 (0.4)	4.3 (2.2)	3.2 (0.5)	6.4 (0.8)	2.3 (0.4)	6.4 (2.9)
T/Thyroid	0.2 (0.1)	0.0 (0.0)	0.2 (0.1)	0.0 (0.0)	0.3 (0.2)	0.1 (0.1)
T/Muscle	7.9 (3.2)	24.5 (27.3)	25.5 (7.4)	48.4 (21.4)	30.5 (7.8)	24.9 (11.6)
T/Blood	1.8 (0.4)	9.0 (5.6)	2.2 (0.3)	8.7 (3.9)	2.7 (0.0)	8.2 (3.9)
T/Ovaries	1.2 (0.1)	3.0 (2.2)	1.7 (0.5)	4.3 (2.1)	1.6 (0.9)	3.3 (2.7)
T/Uterus	2.1 (0.9)	4.8 (3.9)	2.3 (0.6)	1.8 (0.9)	1.4 (0.4)	1.9 (0.8)
Excretion in % ID						
Urine	30.5 (6.5)	67.8 (7.3)	9.7 (5.7)	50.2 (2.1)	28.7 (13.7)	67.5 (12.1)
Faeces	0.0 (0.0)	3.4 (2.1)	0.2 (0.3)	3.2 (0.74)	1.5 (1.0)	6.2 (1.8)

NOTE: The first time point always represents maximum tumor accumulation of each respective format followed by a wash-out time point. Total excretion is measured cumulatively at indicated time points and is calculated as % injected dose. All data are presented as mean values and SD (n = 3).
Abbreviation: ID, injected dose.

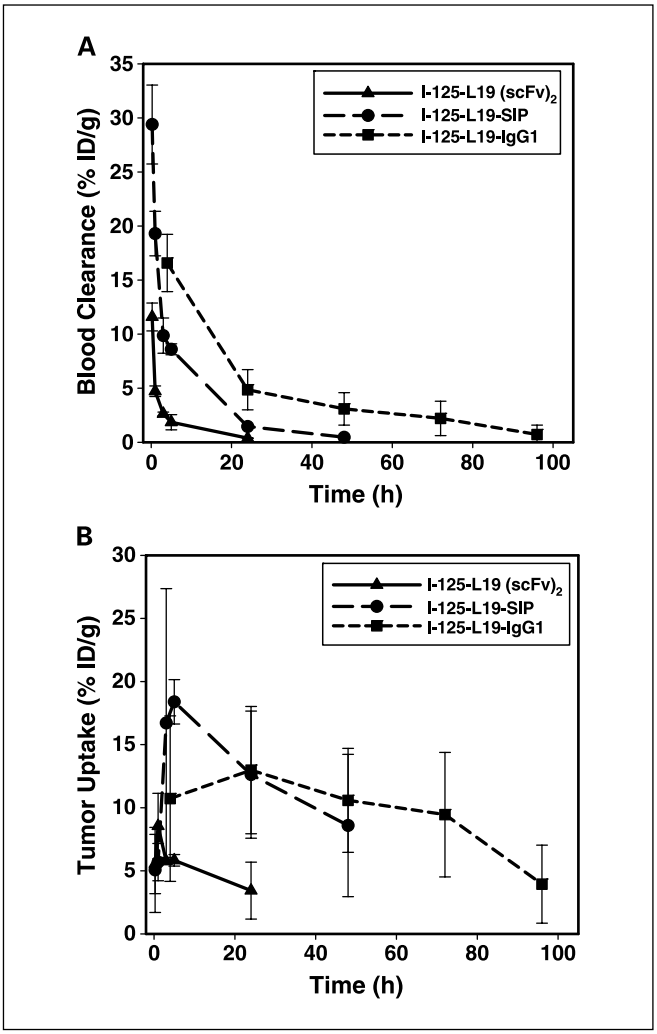

Fig. 4. Uptake and clearance kinetics of different I-125-labeled L19 antibody formats from blood (*A*) and tumor (*B*). Mice bearing F9 tumors were injected i.v. with I-125-L19 (15 kBq), I-125-L19-SIP (34 kBq), or I-125-L19-IgG1 (83 kBq), respectively. Animals injected with iodinated L19 were sacrificed after 0.25, 1, 3, 5, and 24 hours; mice injected with L19-SIP were sacrificed after 0.25, 1, 3, 5, 24, and 48 hours p.i.; and mice injected with L19-IgG1 were killed after 4, 24, 28, 72, and 96 hours p.i. Radioactivity was measured in the blood and the tumor. Mean percentage injected dose per gram of tissue ($n = 3$); bars, ±SD.

separate experiment, the radioiodinated nonbinding small immunoprotein HyHEL-10 (hen egg white lysozyme) was used as the nonspecific control. Criteria to sacrifice the animals were tumor size of >300 mm^2, ulceration of the tumor through the skin and/or body weight loss of >20%. Body weights were collected thrice a week.

Results

Radiolabeling. The radiochemical yields of all radioiodinations ranged between 70% and 90% and the purity of the radiolabeled proteins, as determined by SE-HPLC, was always higher than 90%. The specific activities of the final products ranged from 2 to 6 MBq/nmol for the I-125-labeled derivatives and from ~50 to 100 MBq/nmol for the I-131-labeled immunoconjugates, respectively. Figure 2 shows a representative SE-HPLC chromatogram of I-125-L19-SIP. The SDS-PAGE of I-125-L19-SIP (Fig. 3) revealed only minor amounts of iodinated aggregates or fragments and indicated that the main impurity has approximately half the molecular weight of the iodinated product. This impurity is likely the corresponding monomer resulting from cleavage of the disulfide bridge. For all iodinated L19-bearing proteins the immunoreactivity was higher than 80%.

To radiolabel AP39, L19-SIP, or L19-IgG1 with In-111 the proteins had to be conjugated to a bifunctional metal-chelating moiety. Therefore, MX-DTPA isothiocyanate was reacted with the ε-amine group of lysine residues of the protein. The resulting thio-urea protein-chelator conjugate allowed for easy introduction of the In-111 radiolabel. Incubation at room temperature gave the respective In-111-AP39-MX-DTPA, In-111-L19-SIP-MX-DTPA, and In-111-L19-IgG1-MX-DTPA- radioimmunoconjugates with radiochemical yields ranging from 30% to 60% with specific radioactivity ranging from 2 to 6 MBq/nmol. The radiochemical purity was always higher than 90% and immunoreactivity ranged from 85% to 95%.

Biodistributions. Biodistributions in tumor-bearing mice were carried out up to 24 hours with the small antibody format L19 (AP39), up to 72 hours with the intermediate L19-SIP, and up to 96 hours with the full-size antibody L19-IgG1. Two selected time points of each antibody format either labeled with I-125 or with In-111 via MX-DTPA are listed in Tables 1 and 2. Independent of the format, iodinated antibodies showed increasing thyroid uptake over time (thyroid was not blocked) due to dehalogenation of I-125 *in vivo*. Excretion of the radioactivity was predominantly via the urine (up to ~70% injected dose; Table 1). Whole body elimination and blood clearance were slowest with the full-size antibody format and fastest with the single-chain fragment (Fig. 4A). I-125-L19-SIP showed an intermediate blood and organ clearance and additionally high tumor uptake combined with high tumor-to-tissue ratios (Fig. 4; Table 1). Besides the F9 tumor, specific uptake was found in the ED-B fibronectin–expressing organs ovaries and uterus.

The biodistributions of the In-111-labeled antibodies showed in general a much slower organ and body clearance compared with their I-125-labeled counterparts (Table 2). A particularly high and persistent kidney uptake was found for both of the In-111-labeled antibody fragments, the dimeric single-chain Fv (L19) and the L19-SIP. Whereas the In-111-labeled dimeric single-chain Fv (L19) was rapidly excreted via the urinary pathway (50% injected dose at 24 hours p.i.), the higher molecular weight compounds L19-SIP and L19-IgG1 showed slow excretion in total when labeled with In-111-MX-DTPA. Tumor uptake (in % injected dose/g) was equal or even higher than the iodinated counterparts. However, tumor-to-tissue ratios were significantly lower for all In-111-labeled compounds (Table 2).

Dosimetry of mouse organs. Based on the biodistribution data described above, radiation doses for mouse organs were estimated for the three antibody formats and for both therapeutic isotopes (I-131 and Y-90; Table 3 and 4). For I-131, the calculated doses in the ED-B-expressing tumor and organs (ovaries and uterus), as well as in the non–ED-B-expressing organs increased with the molecular weight of the investigated antibody formats (Table 3). The higher dose in both uterus and ovaries is consistent with known ED-B

fibronectin expression in these organs (32), but only the dose to the ovaries could be critical. However, polyovulating mouse ovaries are not comparable with the human situation and are therefore not considered as dose-limiting organs. For the iodinated dimeric single-chain Fv (L19), the kidneys were the dose-limiting organ when related to the human tolerance dose ($TD_{50/5}$ = 25 Gy). It was calculated that 94 MBq of I-131-L19 could be injected per mouse to achieve this kidney dose. This MTA would result in a tumor dose of 25 Gy for a 100-mg F9 tumor. The red marrow ($TD_{50/5}$ = 4.5 Gy) was the dose-limiting organ in case of the L19-SIP and the L19-IgG1. Corresponding MTAs per mouse were ~71 MBq for the I-131-L19-SIP and 24 MBq for I-131-L19-IgG1, resulting in F9 tumor doses of 66 and 27 Gy, respectively. The dose ratio between the dose-limiting organ and F9 tumor (100 mg) here defined as the therapeutic index was highest for the I-131-L19-SIP with a factor of 14.7 (Fig. 5A). For the respective Y-90-labeled antibody formats, significantly higher organ doses and higher tumor doses were found compared with the iodinated counterparts (Table 4). The kidneys were determined to be the dose-limiting organ in case of the dimeric single-chain Fv Y-90-MX-DTPA-AP39 and the Y-90-MX-DTPA-L19-SIP resulting in MTAs of 3 and 4 MBq, respectively. For the Y-90-MX-DTPA-L19-IgG1, again the red marrow was the dose-limiting organ with a maximum activity of 7 MBq to be injected per mouse. The dose ratios for the therapeutic index (Fig. 5B) of the Y-90 antibody formats were therefore much lower compared with the iodinated antibody formats.

Myelotoxicity. Blood cell counts were done in non-tumor-bearing mice injected with increasing doses of I-131-L19-SIP or I-131-L19-IgG1. 37 MBq and 74 MBq of L19-SIP (the approximate MTA, based on dosimetry), and 25 MBq (the approximate MTA, based on dosimetry) and 74 MBq of L19-IgG1 were administered. 74 MBq L19-IgG1 was chosen as a second dose group with expected severe bone marrow toxicity. Figure 6 shows the blood cell counts at the respective doses. The nadirs of leukocyte counts depending on the dose were reached at 1 to 2 weeks after antibody administration. At the respective MTAs for I-131-labeled L19-SIP and L19-IgG1, the severity of the myelotoxicity was not significantly different for both antibody formats (Fig. 6A). However, recovery from myelotoxicity was faster for the L19-SIP (~3 weeks p.i.) compared to the L19-IgG1 (4-5 weeks p.i.).

Table 2. Biodistribution of In-111-labeled anti-ED-B antibody formats in F9 tumor-bearing mice each at two selected time points

Formats	AP39 sc(Fv)$_2$, mean (SD)		L19-SIP, mean (SD)		L19-IgG1, mean (SD)	
Time points	1 h	24 h	4 h	24 h	24 h	96 h
Uptake in % ID/g						
Spleen	1.9 (0.5)	1.2 (0.2)	4.1 (0.2)	3.7 (0.5)	8.1 (3.8)	7.2 (0.7)
Liver	2.6 (1.3)	2.3 (0.8)	6.4 (0.3)	7.1 (1.0)	6.1 (2.4)	3.3 (0.4)
Kidneys	66.9 (8.2)	44.0 (3.4)	22.9 (2.4)	32.1 (2.9)	6.0 (0.8)	1.7 (0.4)
Lung	1.5 (1.6)	0.8 (0.2)	8.2 (0.4)	3.5 (0.6)	2.0 (0.7)	0.7 (0.2)
Bone	3.0 (0.5)	1.6 (0.2)	5.5 (1.1)	8.0 (1.5)	10.9 (2.8)	4.0 (1.3)
Thyroid	7.9 (8.6)	1.7 (1.1)	8.7 (3.9)	3.9 (1.4)	1.9 (0.7)	1.1 (0.2)
Muscle	3.4 (4.5)	0.4 (0.1)	1.0 (0.1)	1.1 (0.1)	0.4 (0.1)	0.3 (0.2)
Tumor	12.9 (4.8)	4.3 (0.8)	16.7 (5.2)	14.3 (1.5)	12.0 (1.9)	4.9 (0.9)
Blood	5.6 (1.9)	0.1 (0.0)	9.4 (0.4)	1.9 (0.2)	2.3 (1.2)	0.3 (0.2)
Ovaries	4.6 (1.5)	2.5 (0.3)	25.8 (6.9)	11.7 (4.8)	9.5 (2.2)	5.4 (1.1)
Uterus	8.6 (11.8)	4.3 (1.5)	10.1 (4.5)	18.0 (1.9)	7.9 (7.4)	7.8 (3.0)
Tumor/Tissue ratios						
T/Spleen	7.4 (4.6)	3.7 (0.2)	4.1 (1.4)	3.9 (0.4)	1.7 (1.3)	0.7 (0.1)
T/Liver	7.2 (7.0)	2.0 (0.6)	2.6 (0.9)	2.0 (0.1)	2.2 (1.1)	1.5 (0.3)
T/Kidneys	0.2 (0.1)	0.1 (0.0)	0.8 (0.3)	0.5 (0.1)	2.1 (0.6)	2.9 (0.2)
T/Lung	17.6 (13.3)	5.8 (1.0)	2.0 (0.6)	4.2 (0.3)	6.2 (1.7)	7.4 (1.0)
T/Bone	4.5 (2.2)	2.7 (0.2)	3.1 (1.1)	1.8 (0.4)	1.2 (0.4)	1.3 (0.2)
T/Thyroid	2.7 (1.7)	3.2 (1.5)	2.2 (1.3)	4.0 (1.2)	7.1 (3.1)	4.6 (1.0)
T/Muscle	9.8 (7.1)	9.9 (1.4)	16.5 (3.6)	12.8 (1.8)	30.7 (12.1)	19.5 (10.3)
T/Blood	2.8 (2.0)	38.4 (3.8)	1.8 (0.6)	7.6 (0.8)	6.4 (3.1)	17.5 (5.5)
T/Ovaries	3.0 (1.5)	1.8 (0.4)	0.7 (0.4)	1.3 (0.4)	1.3 (0.3)	0.9 (0.1)
T/Uterus	4.2 (3.2)	1.1 (0.3)	1.8 (0.7)	0.8 (0.0)	2.6 (1.8)	0.7 (0.2)
Excretion in % ID						
Urine	19.0 (16.8)	50.3 (5.3)	5.5 (1.1)	20.3 (5.1)	14.9 (4.5)	52.7 (3.2)
Faeces	2.0 (1.9)	5.1 (3.5)	0.5 (0.4)	4.1 (2.0)	2.6 (0.7)	14.6 (2.2)

NOTE: The first time point always represents maximum tumor accumulation of the respective format followed by a wash-out time point. Total excretion is measured cumulatively at indicated time points and is calculated as % injected dose. All data are presented as mean values and SD (n = 3).
Abbreviation: ID, injected dose.

Table 3. Doses delivered to mouse organs and F9 tumor (100 mg) calculated for the therapeutic isotope I-131 based on biodistributions with three I-125-labeled anti-ED-B antibody formats (mGy/MBq)

Organ, I-131	Mouse organ doses (mGy/MBq)		
	L19 ($scFv)_2$	L19-SIP	L19-IgG1
Spleen	15	61	163
Liver	7	50	170
Kidneys	265	160	315
Lung	79	176	560
Red Marrow	14	63	186
Ovaries	517	586	664
Uterus	133	959	1,019
F9 Tumor (100 mg)	264	925	1,135
MTA (MBq)	94	71	24
F9 Tumor Dose (Gy)	25	66	27

NOTE: The dose to a F9 tumor (100 mg) after injection of the maximum tolerated activity is additionally presented for the three I-125-labeled anti-ED-B antibody formats (Gy).

The number of thrombocytes returned 1 week earlier into the reference range than the leukocytes (Fig. 6B). In the group of animals receiving 37 MBq of I-131-L19-SIP, no significant drop beneath the reference range of leukocytes as well as thrombocyte counts was detected. After injection of 74 MBq I-131-L19-IgG1, severe toxicity to the mice was found in terms of rapid body weight loss of >20% and dramatic decrease of leukocytes and thrombocytes counts after 1 week. The bone marrow damage due to radiation was irreversible and resulted in death of all animals. The results of these myelotoxicity studies confirmed the calculated MTAs for I-131-labeled L19-SIP and L19-IgG1 with the red bone marrow as the dose-limiting organ in a radioimmunotherapeutic setting.

Table 4. Doses delivered to mouse organs and F9 tumor (100 mg) calculated for the therapeutic isotope Y-90 based on biodistributions with three In-111-labeled anti-ED-B antibody formats (mGy/MBq)

Organ, Y-90	Mouse organ doses (mGy/MBq)		
	AP39 $sc(Fv)_2$	L19-SIP	L19-IgG1
Spleen	123	557	1,370
Liver	466	1,489	1,699
Kidneys	10,153	6,876	1,620
Lung	265	1,042	757
Thyroid	333	462	321
Red Marrow	39	211	635
Ovaries	232	1,293	1,465
Uterus	921	1,972	2,141
F9 Tumor(100 mg)	578	1,925	1,720
MTA (MBq)	3	4	7
F9 Tumor Dose (Gy)	1	7	12

NOTE: The dose to a F9 tumor (100 mg) after injection of the maximum tolerated activity is additionally presented for the three In-111-labeled anti-ED-B antibody formats (Gy).

Radioimmunotherapy. Radioimmunotherapy with a single injection of I-131-L19-SIP (37-74 MBq) showed a dose-dependent effect on the growth of F9 tumors in mice (Fig. 7). Treatment with the MTA of 74 MBq I-131-L19-SIP (determined by dosimetry calculations and myelotoxicity studies; as described before) led to a stasis of tumor growth for 10 days (Fig. 7A). Median survival after high-dose treatment (74 MBq) was 22 versus 15 days for mice treated with 37 MBq and 9 days for untreated controls (Fig. 7B). In all groups, body weight loss did not exceed 5%. In a separate control experiment using the unspecific small immunoprotein HyHEL-10, no therapeutic effect on F9 tumor growth could be observed (data not shown). Survival of the animals injected with 64 MBq I-131-HyHEL-10 was identical to untreated control animals. A tumor regression study was also done with the I-131-radiolabeled L19-IgG1 in the F9 tumor model. The MTA of I-131-L19-IgG1 was determined to be 25 MBq. Given as a single injection, 25 MBq I-131-L19-IgG1 led to slower tumor growth and a 7-day prolongation of survival compared to the untreated controls (Fig. 8). No loss in body weight was observed.

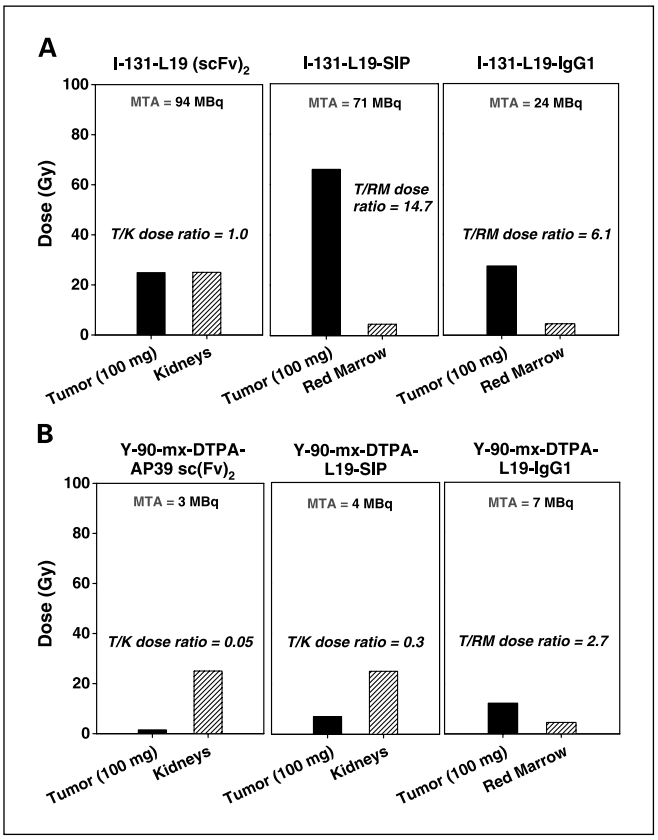

Fig. 5. Therapeutic index given as the ratio between F9 tumor and dose-limiting organ doses for I-131-labeled (*A*) and Y-90-labeled (*B*) anti-ED-B antibody formats. Dose-limiting organs (either kidney or red marrow) were determined by reference to known human tolerance dose ($TD_{50/5}$) values. The F9 tumor dose was calculated for a tumor mass of 100 mg. The MTA, (given in MBq) corresponds to the amount of injected activity that delivers the $TD_{50/5}$ to the dose-limiting organ.

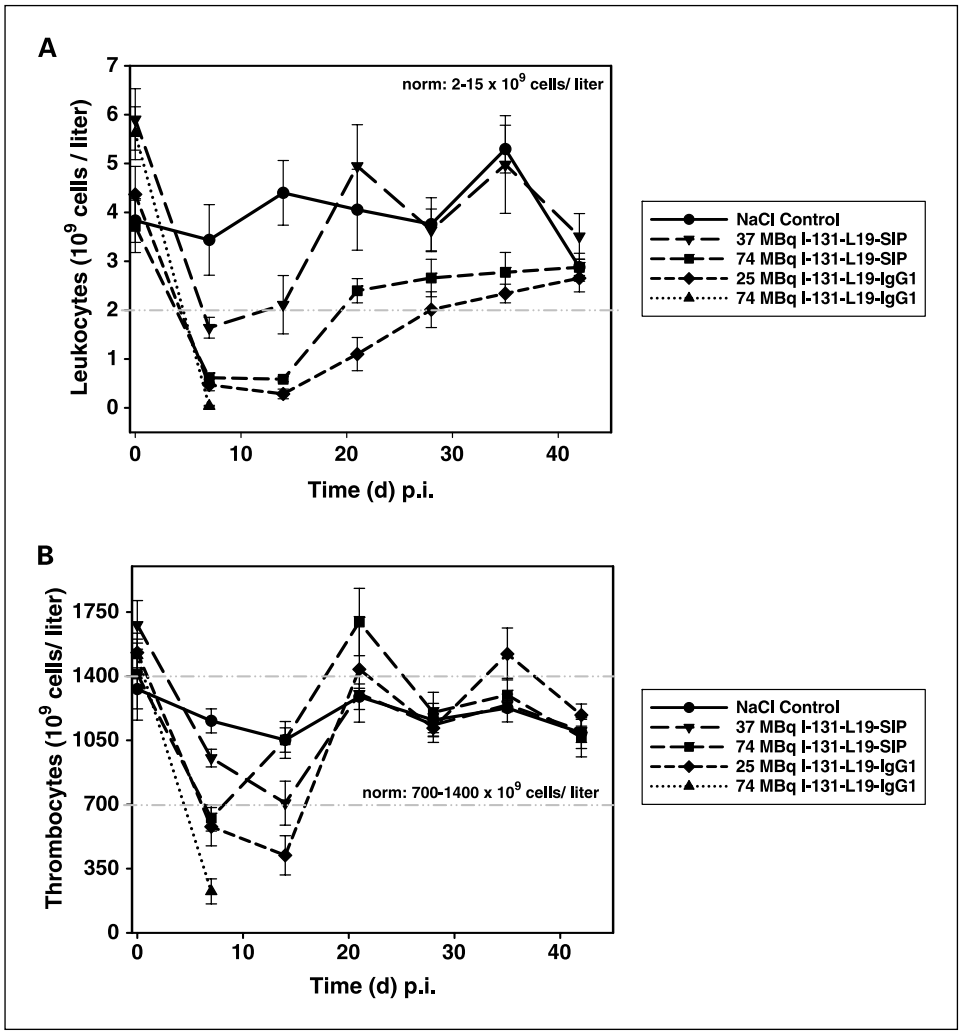

Fig. 6. Myelotoxicity in non-tumor–bearing mice after single administration of different doses I-131-L19-SIP (37 and 74 MBq) and I-131-L19-IgG1 (25 and 74 MBq). The blood cell counts were determined weekly for 6 weeks. *A*, leukocytes; *B*, thrombocytes. Mean ($n = 6$); bars, ±SE.

Discussion

In the present study, different formats of the anti-ED-B fibronectin antibody L19 (dimeric single-chain Fv, SIP, and IgG1) have been investigated after radioiodination and radiometal labeling. All tested L19-based radioimmunoconjuagtes displayed good targeting of ED-B fibronectin expressing tissues (i.e., tumor, uterus, and ovaries) in biodistribution studies. ED-B fibronectin expression in F9 tumors as well as in uterus and ovaries has been reported earlier (14, 32). As expected, based on their molecular weights, elimination from normal organs and whole body was slowest with the IgG1 and fastest with the dimeric single-chain Fv (Tables 1 and 2). In general, In-111-labeled anti-ED-B antibodies (labeled via MX-DTPA) showed significantly slower organ and whole body clearance compared with their I-125-labeled counterparts (Tables 1 and 2). In particular, the In-111-labeled derivatives AP39 and L19-SIP showed a high and persistent kidney uptake as documented for other radiometal-labeled antibody fragments (33, 34). Previous studies have already shown that In-111-labeled DTPA-conjugated antibody fragments (via lysine residues) were degraded to a DTPA-ε-amino-lysine derivative, which is retained in the lysosomes of the kidneys (35). In contrast to In-111-labeled L19-SIP, its I-125-labeled counterpart did not show such a high and persistent kidney retention. This result is in agreement with a report of Yazaki et al. (36) who made the same observation when they had investigated the biodistribution of an anti-carcinoembryonic antigen antibody fragment of similar size after I-125 and In-111 labeling.

For radiolabeled antibodies and antibody fragments used for radioimmunotherapy, the ionizing dose that can be administered is limited by the dose tolerated by normal organs and tissues. By making dose estimates based on biodistribution studies, critical organs can be determined before therapy. By this means, safe activity doses can be calculated either for patients or for animals. In addition, a certain range of effectiveness to the tumor can be predicted, which is needed for individual treatment planning and patient management. In our animal study, we decided in particular not to pursue Y-90-labeled antibody formats for tumor therapy, because based on medical internal radiation dose dosimetry, I-131-labeled antibodies seemed much more promising in terms of mouse organ doses and doses delivered to the tumor after injection of the MTA (Tables 3 and 4). However, it has to be considered that dosimetry based on medical internal radiation dose is very limited as it uses several simplified assumptions such as an homogenous organ or tumor distribution of the labeled compound (28).

In addition, this principle is considered for human use but not for animals. Only a few reports described mouse dosimetry models and mouse *S*-values taking only a few isotopes and some selected organs into account (37–39). An extensive, user-friendly software does not exist for animals thus far. Other difficulties in mouse dosimetry reveal for example the cross-fire effect, which is especially important for Y-90 due to its long range of β particles but relatively small size of mouse organs. However, the cross-fire effect of Y-90-labeled antibodies was not considered in our study. For the short-range β particles of I-131, the cross-fire effect in mice is less important. The dose-limiting toxicity of radioimmunoconjugates is in most cases either hematopoietic suppression resulting from the marrow radiation exposure associated with the circulation time of the radioimmunoconjugate (40) or nephrotoxicity due to high uptake and retention of the radioimmunoconjugate in the kidneys (41). Concerning the bone marrow toxicity of radioimmunoconjugates, it should be mentioned that the calculation of human red marrow doses is still under debate. Several methods have been tested thus far without a final consensus (28, 42–44). Nevertheless, our mouse dosimetry results regarding the predicted bone marrow MTAs for I-131-L19-SIP and I-131-L19-IgG1 were confirmed by the myelotoxicity study, because after injection of the predicted MTA, a reversible decrease of both leukocytes and thrombocytes below normal was observed for both radioimmunoconjugates (Fig. 6a and b). These results show the predictive power and usefulness of the dosimetric calculations.

The most favorable therapeutic index (dose ratio between the F9 tumor and the dose-limiting organ) was observed for I-131-L19-SIP (Fig. 5a and b). Therefore, higher doses to the tumor can be safely delivered by I-131-L19-SIP compared with the other investigated radioimmunoconjugates. The better performance of I-131-L19-SIP compared with I-131-L19-IgG1 could also be shown by improved therapeutic efficacy (Figs. 7 and 8). The question of which format should be used for radioimmunotherapy was often addressed using different targets and different radioimmunoconjugates (45, 46) but still remains unsolved. Additionally, therapeutic isotopes were compared at their MTAs to find the most suited dose rate and effectiveness (47, 48). Whereas some have recommended iodinated Fab fragments (47), we came to the conclusion that the I-131-labeled small immunoprotein is the most suitable radioimmunoconjugate for ED-B fibronectin–targeted radioimmunotherapy. Cure of tumor-bearing animals was not achieved, which might be influenced by several factors. First, the F9 teratocarcinoma is a very aggressive tumor (doubling time ~48 hours) and therapy studies were started with already palpable tumors of ~80 mm^2 in size. Second, neither dose fractionation nor repeated injections after recovery from toxic side effects were tested here. Dose fractionation as well as repeated injections of

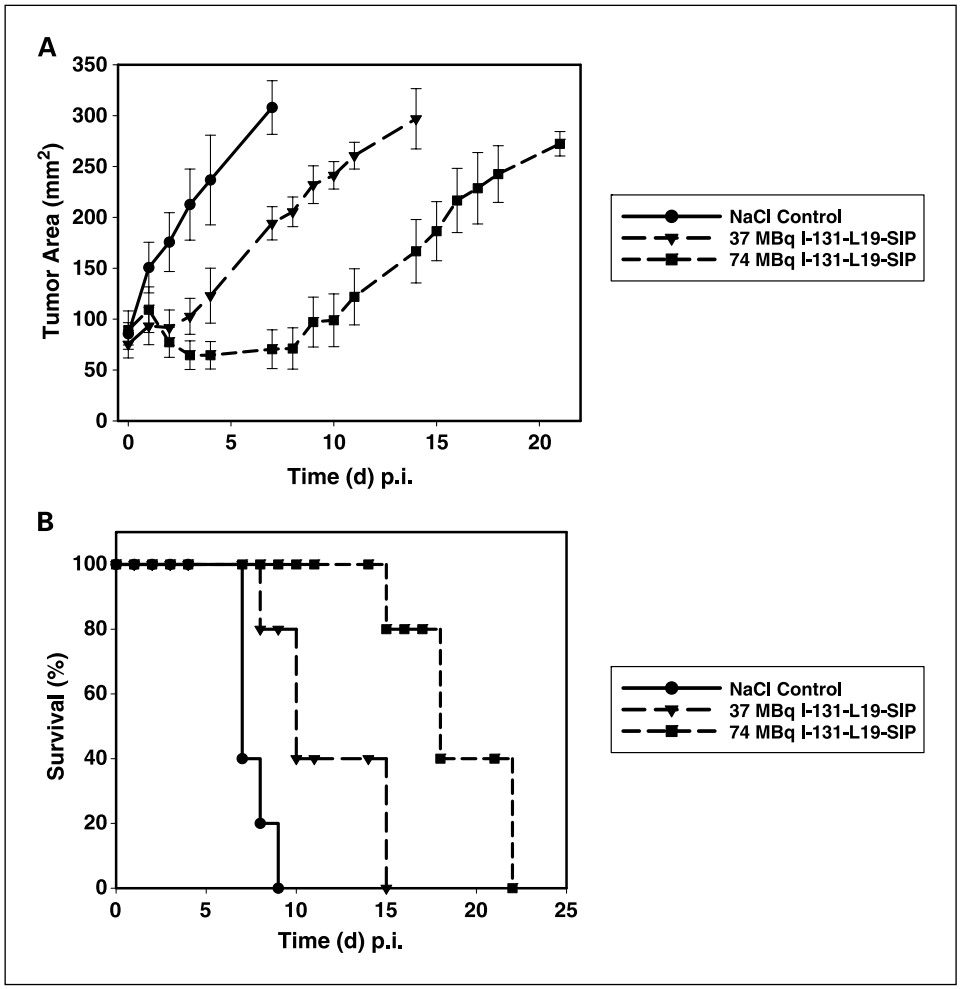

Fig. 7. Tumor growth (*A*) and survival (*B*) curves of F9 tumor-bearing mice treated with I-131-L19-SIP given as a single injection of either 37 or 74 MBq compared with control animals injected with saline. Mean tumor area (tumor growth, $n = 5$); bars, ±SE.

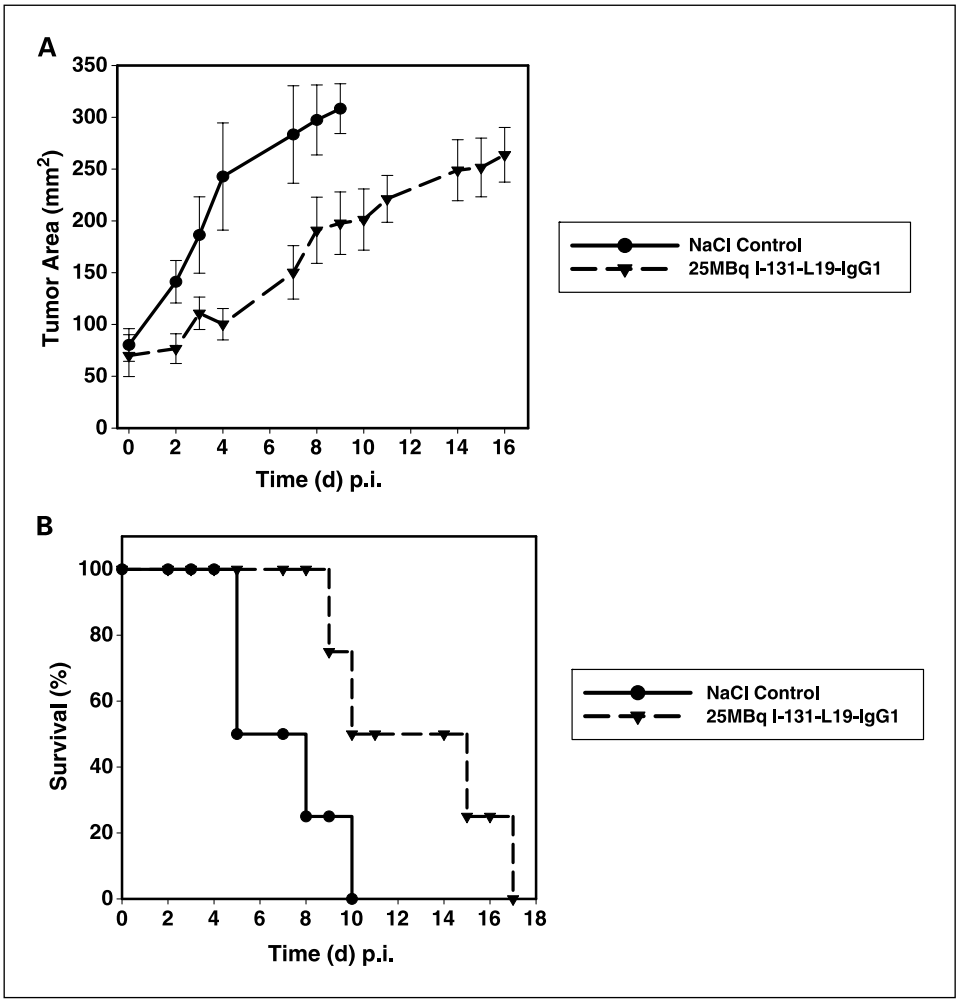

Fig. 8. Tumor growth (*A*) and survival (*B*) curves of F9 tumor-bearing mice treated with I-131-L19-IgG1 given as single injection of 25 MBq compared with control animals injected with saline. Mean tumor area (tumor growth, $n = 8$); bars, ±SE.

radioimmunoconjugates given at their maximum tolerated doses have been reported to improve the prospects of radioimmunotherapy significantly (49–51).

In conclusion, the results presented in this report suggest a new avenue for the treatment of cancer in patients by ED-B fibronectin-targeted radioimmunotherapy. Based on animal experiments, we have identified the I-131-labeled human SIP as the best-suited antibody format for ED-B-targeted radioimmunotherapy when compared with I-131-labeled dimeric single-chain Fv and IgG1 formats, as well as Y-90-labeled dimeric single-chain Fv, SIP, and IgG1. The administration of I-131-labeled ED-B fibronectin-binding L19-SIP led to an effective tumor growth delay and prolonged survival in an extremely aggressive tumor model without causing severe side-effects. This novel radioimmunoconjugate could potentially be used for the treatment of solid cancers.

Acknowledgments

We thank Melanie Appel, Ingo Horn, Joerg Pioch, Volker Stickel, Ingolf Weber, and Simone Zolchow for excellent technical assistance and Dieter Moosmayer and Guido Malawski for production and purification of the AP39 antibody fragment.

References

1. Vose JM. Antibody-targeted therapy for low-grade lymphoma. Semin Hematol 1999;36:15–20.
2. Goldenberg DM. The role of radiolabeled antibodies in the treatment of non-Hodgkin's lymphoma: the coming of age of radioimmunotherapy. Crit Rev Oncol Hematol 2001;39:195–201.
3. Jain RK. Physiological barriers to delivery of monoclonal antibodies and other macromolecules in tumors. Cancer Res 1990;50:814–9s.
4. Yokota T, Milenic DE, Whitlow M, Schlom J. Rapid tumor penetration of a single-chain Fv and comparison with other immunoglobulin forms. Cancer Res 1992;52:3402–8.
5. Paganelli G, Magnani P, Zito F, et al. Three-step monoclonal antibody targeting in carcinoembryonic antigen-positive patients. Cancer Res 1991;51:5960–6.
6. Barbet J, Kraeber-Bodere F, Vuillez JP, Gautherot E, Rouvier E, Chatal JF. Pretargeting with the affinity enhancement system for radioimmunotherapy. Cancer Biother Radiopharm 1999;14:153–66.
7. Breitz HB, Weiden PL, Beaumier PL, et al. Clinical optimization of pretargeted radioimmunotherapy with antibody-streptavidin conjugate and ^{90}Y-DOTA-biotin. J Nucl Med 2000;41:131–40.
8. Imam SK. Status of radioimmunotherapy in the new millenium. Cancer Biother Radiopharm 2001;16:237–56.
9. Zardi L, Carnemolla B, Siri A, et al. Transformed human cells produce a new fibronectin isoform by preferential alternative splicing of a previously unobserved exon. EMBO J 1987;6:2337–42.
10. Carnemolla B, Neri D, Castellani P, et al. Phage antibodies with pan-species recognition of the oncofoetal angiogenesis marker fibronectin ED-B domain. Int J Cancer 1996;68:397–405.
11. Neri D, Carnemolla B, Nissim A, et al. Targeting by affinity-matured recombinant antibody fragments of an angiogenesis associated fibronectin isoform. Nat Biotechnol 1997;15:1271–5.
12. Pini A, Viti F, Santucci A, et al. Design and use of a phage display library. Human antibodies with subnanomolar affinity against a marker of angiogenesis

eluted from a two-dimensional gel. J Biol Chem 1998; 273:21769–76.
13. Viti F, Tarli L, Giovannoni L, Zardi L, Neri D. Increased binding affinity and valence of recombinant antibody fragments lead to improved targeting of tumoral angiogenesis. Cancer Res 1999;59:347–52.
14. Tarli L, Balza E, Viti F, et al. A high-affinity human antibody fragment that targets tumoral blood vessels. Blood 1999;94:192–8.
15. Santimaria M, Moscatelli G, Viale GL, et al. Immunoscintigraphic detection of the ED-B domain of fibronectin, a marker of angiogenesis, in patients with cancer. Clin Cancer Res 2003;9:571–9.
16. Birchler M, Viti F, Zardi L, Spiess B, Neri D. Selective targeting and photocoagulation of ocular angiogenesis mediated by a phage-derived human antibody fragment. Nat Biotechnol 1999;17:984–8.
17. Nilsson F, Kosmehl H, Zardi L, Neri D. Targeted delivery of tissue factor to the ED-B domain of fibronectin, a marker of angiogenesis, mediates the infarction of solid tumors in mice. Cancer Res 2001;61:711–6.
18. Carnemolla B, Borsi L, Balza E, et al. Enhancement of the antitumor properties of interleukin-2 by its targeted delivery to the tumor blood vessel extracellular matrix. Blood 2002;99:1659–65.
19. Halin C, Rondini S, Nilsson F, et al. Enhancement of the antitumor activity of interleukin-12 by targeted delivery to neovasculature. Nat Biotechnol 2002;20:264–9.
20. Borsi L, Balza E, Carnemolla B, et al. Selective targeted delivery of TNFα to tumor blood vessels. Blood 2003;102:4384–92.
21. Borsi L, Balza E, Bestagno M, et al. Selective targeting of tumoral vasculature: comparison of different formats of an antibody (L19) to the ED-B domain of fibronectin. Int J Cancer 2002;102:75–85.
22. Scheuermann J, Viti F, Neri D. Unexpected observation of concentration-dependent dissociation rates for antibody-antigen complexes and other macromolecular complexes in competition experiments. J Immunol Methods 2003;276:129–34.
23. Fraker PJ, Speck JC. Protein and cell membrane iodinations with a sparingly soluble chloramide 1,3,4,6-tetrachloro-3α-6α-diphenylglycouril. Biochem Biophys Res Commun 1978;80:849–57.
24. Birchler M, Neri G, Tarli L, Halin C, Viti F, Neri D. Infrared photodetection for the *in vivo* localization of phage-derived antibodies directed against angiogenic markers. J Immunol Methods 1999;231:239–48.
25. Brechbiel MW, Gansow OA. Backbone-substituted DTPA-ligands for Y-90 radioimmunotherapy. Bioconjugate Chem 1991;2:187–94.
26. Lehmann L, Suelzle D, Friebe M, Brumby T, Platzek J. inventors; Schering AG, assignee. Conjugate enantiomerically pure (4*S*,8*S*)- and (4*R*, 8*R*)-4-*p*-benzyl-8-methyl-3,6,9-triaza-3*N*,6*N*,9*N*-tricarboxymethyl-1, 11-undecanoic acid and their metal complexes with biomolecules, procedure for their production and use in radiodiagnostics and radiotherapy. Germany patent DE 10305463 A1 20040812; 2003.
27. Borsi L, Carnemolla B, Balza E, et al. inventors; Philogen S.r.L, Schering AG, assignees. Selective targeting of tumor vasculature using anti-fibronectin antibodies. PCT International patent application WO 2003076469 A2 20030918; 2003.
28. Loevinger R, Budinger T, Watson E. MIRD Primer for absorbed dose calculations. New York: Society of Nuclear Medicine; 1988.
29. Siegel JA, Thomas SR, Stubbs JB, et al. MIRD Pamphlet No. 16: techniques for quantitative radiopharmaceutical biodistribution data acquisition and analysis for use in human radiation dose estimates. J Nucl Med 1999;40:37–61S.
30. Sgouros G. Bone marrow dosimetry for radioimmunotherapy: theoretical considerations. J Nucl Med 1993;34:689–94.
31. Pizarello DJ, Witcofski RL. Medical radiation biology. Philadelphia: Lea & Febiger; 1982.
32. Carnemolla B, Balza E, Siri A, et al. A tumor-associated fibronectin isoform generated by alternative splicing of messenger RNA precursors. J Cell Biol 1989; 108:1139–48.
33. Tahtis K, Lee FT, Smyth FE, et al. Biodistribution properties of In-111-labeled C-functionalized *trans*-cyclohexyl diethylenetriaminepentaacetic acid humanized 3S193 diabody and F(ab′)2 constructs in a breast carcinoma xenograft model. Clin Cancer Res 2001;7: 1061–72.
34. Colcher D, Goel A, Pavlinkova G, Beresford G, Booth B, Batra SK. Effects of genetic engineering on the pharmacokinetics of antibodies. Q J Nucl Med 1999;43:132–9.
35. Rogers BE, Franano FN, Duncan JR, et al. Identification of metabolites of 111In-diethylenetriaminepentaacetic acid-monoclonal antibodies and antibody fragments *in vivo*. Cancer Res 1995;55:5714–20s.
36. Yazaki PJ, Wu AM, Tsai S, et al. Tumor targeting of radiometal labeled anti-CEA recombinant T84.66 diabody and T84.66 minibody: comparison to radioiodinated fragments. Bioconjugate Chem 2001;12:220–8.
37. Hui TE, Fisher DR, Kuhn JA, et al. A mouse model for calculating cross-organ β doses from Yttrium-90-labeled immunoconjugates. Cancer (Suppl) 1994;73: 951–7.
38. Flynn AA, Green AJ, Pedley RB, Boxer GM, Boden R, Begent RHJ. A mouse model for calculating the absorbed β-particle dose from I-131- and Y-90-labeled immunoconjugates, including a method for dealing with heterogeneity in kidney and tumor. Radiation Res 2001;156:28–35.
39. Kolbert KS, Watson T, Matei C, Xu S, Koutcher JA, Sgouros G. Murine S factors for liver, spleen, and kidney. J Nucl Med 2003;44:784–91.
40. Bander NH, Nanus DM, Milowsky MI, Kostakoglu L, Vallabhajosula S, Goldsmith SJ. Targeted systemic therapy of prostate cancer with a monoclonal antibody to prostate-specific membrane antigen. Semin Oncol 2003;30:667–77.
41. Adams GP, Shaller CC, Dadachova E, et al. A single treatment of yttrium-90 labeled CHX-A″-C6.5 diabody inhibits the growth of established human tumor xenografts in immunodeficient mice. Cancer Res 2004;64:6200–6.
42. Siegel JA, Yeldell D, Goldenberg DM, et al. Red marrow radiation dose adjustment using plasma FLT3-L cytokine levels: improved correlations between hematologic toxicity and bone marrow dose for radioimmunotherapy patients. J Nucl Med 2003; 44:67–76.
43. O'Donoghue JA, Baidoo NE, Deland D, Welt S, Divgi CR, Sgouros G. Hematologic toxicity in radioimmunotherapy: dose-response relationships for I-131 labeled antibody therapy. Cancer Biother Radiopharm 2002; 17:435–43.
44. DeNardo GL, HartmannSiantar CL, DeNardo SJ. Radiation dosimetry for radionuclide therapy in a nonmyeloablative strategy. Cancer Biother Radiopharm 2002;17:107–18.
45. Hudson PJ. Recombinant antibody constructs in cancer therapy. Curr Opin Immunol 1999;11: 548–57.
46. Behr TM, Memtsoudis S, Sharkey RM, et al. Experimental studies on the role of antibody fragments in cancer radio-immunotherapy: influence of radiation dose and dose rate on toxicity and anti-tumor efficacy. Int J Cancer 1998;77:787–95.
47. Brouwers AH, van Eerd JEM, Frielink C, et al. Optimization of radioimmunotherapy of renal cell carcinoma: labeling of monoclonal antibody cG250 with I-131, Y-90, Lu-177, or Re-186. J Nucl Med 2004;45: 327–37.
48. Behr TM, Béhe M, Loehr M, et al. Therapeutic advantages of Auger electron- over β-emitting radiometals or radioiodine when conjugated to internalizing antibodies. Eur J Nucl Med 2000;27:753–65.
49. Vallabhajosula S, Smith-Jones PM, Navarro V, Goldsmith SJ, Bander NH. Radioimmunotherapy of prostate cancer in human xenografts using monoclonal antibodies specific to prostate specific membrane antigen (PSMA): studies in nude mice. Prostate 2004; 58:145–55.
50. DeNardo GL, Schlom J, Buchsbaum DJ, et al. Rationales, evidence, and design considerations for fractionated radioimmunotherapy. Cancer (Suppl) 2002;94:1332–48.
51. Blumenthal RD, Alisauskas R, Juweid M, Sharkey RM, Goldenberg DM. Defining the optimal spacing between repeat radioantibody doses in experimental models. Cancer (Suppl) 1997;80:2624–35.

Clinical Cancer Research

Radioimmunotherapy of Solid Tumors by Targeting Extra Domain B Fibronectin: Identification of the Best-Suited Radioimmunoconjugate

Dietmar Berndorff, Sandra Borkowski, Stephanie Sieger, et al.

Clin Cancer Res 2005;11:7053s-7063s.